Accepted Manuscript

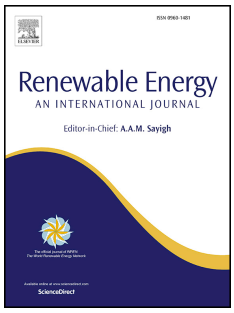

Eigen-analysis of hydraulic-mechanical-electrical coupling mechanism for small signal stability of hydropower plant

Weijia Yang, Per Norrlund, Chi Yung Chung, Jiandong Yang, Urban Lundin

PII: S0960-1481(17)30757-7

DOI: 10.1016/j.renene.2017.08.005

Reference: RENE 9102

To appear in: *Renewable Energy*

Received Date: 14 January 2017

Revised Date: 17 July 2017

Accepted Date: 3 August 2017

Please cite this article as: Yang W, Norrlund P, Chung CY, Yang J, Lundin U, Eigen-analysis of hydraulic-mechanical-electrical coupling mechanism for small signal stability of hydropower plant, *Renewable Energy* (2017), doi: 10.1016/j.renene.2017.08.005.

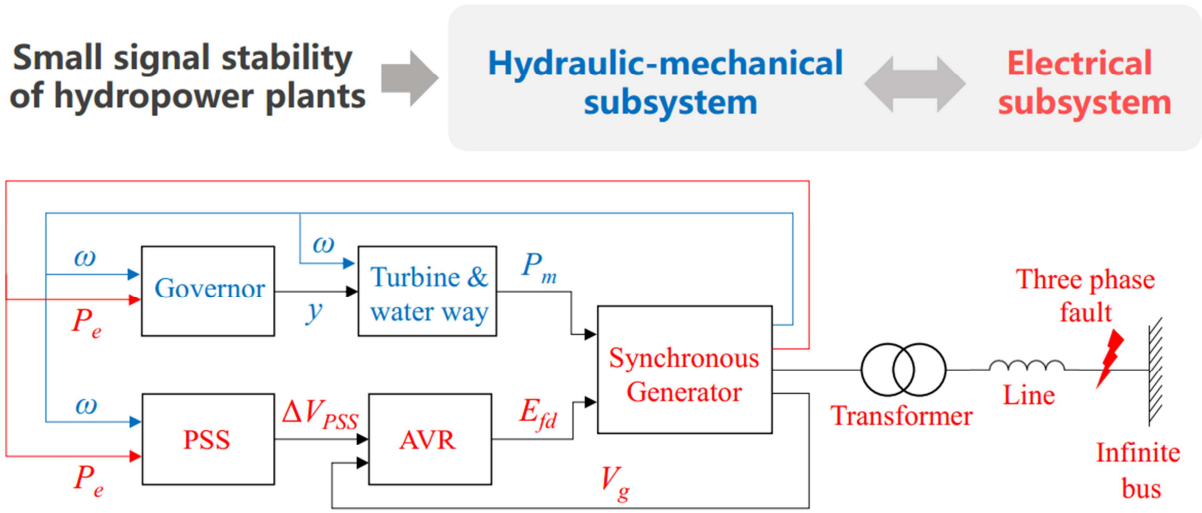

Eigen-analysis of hydraulic-mechanical-electrical coupling mechanism for small signal stability of hydropower plant

Weijia Yang [a,b,*1], Per Norrlund [a,c], Chi Yung Chung [d], Jiandong Yang [b], Urban Lundin [a]

[a] Division of Electricity, Department of Engineering Sciences, Uppsala University, Uppsala, SE-751 21, Sweden

[b] The State Key Laboratory of Water Resources and Hydropower Engineering Science, Wuhan University, Wuhan, 430072, China

[c] Vattenfall R&D, Älvkarleby, SE-814 26, Sweden

[d] Department of Electrical and Computer Engineering, University of Saskatchewan, Saskatoon, SK S7N 5A9, Canada

Abstract. Hydropower shoulders important responsibility for regulation and control of power systems with intermittent renewable energy sources. The quality of regulation required for hydropower units has been increasing, and the interaction between hydropower plants (HPPs) and power systems is of great importance. This work aims to conduct a fundamental study on hydraulic-mechanical-electrical coupling mechanism for small signal stability of HPPs. The main focus is the impact of hydraulic-mechanical factors on the local mode oscillation in a Single-Machine-Infinite-Bus system. A twelfth-order state matrix is established for theoretical eigen-analysis as the core approach. Meanwhile, a simulation model based on Simulink/SimPowerSystems is built for validation. The influencing mechanisms of water column elasticity, governor mechanical component, and water inertia are studied under different control modes of the turbine governor. The results show considerable influence from hydraulic-mechanical factors, and the effect of turbine governor actions is no longer ignorable; also, the damping performance

* Corresponding author.

E-mail addresses: weijia.yang@angstrom.uu.se (W. Yang), per.norrlund@vattenfall.com (P. Norrlund), c.y.chung@usask.ca (C. Y. Chung), jdyang@whu.edu.cn (J. Yang), Urban.Lundin@angstrom.uu.se, (U. Lundin).

under power system stabilizers can be considerably affected. Insights into interactions among physical quantities in various conditions are obtained as well.

Key words: small signal stability; hydropower plant; turbine governor; eigenvalue; power system stabilizer

Nomenclature

Symbol	Unit	Description
b_p	[pu]	turbine governor parameter: for droop
c	[m/s]	pressure propagation speed in penstock
e_{qy} ,$e_{q\omega}$,e_{qh}	[pu]	partial derivative of turbine discharge with respect to guide vane opening, speed and head
e_y ,e_ω ,e_h	[pu]	partial derivative of turbine power output with respect to guide vane opening, speed and head
E_q'	[pu]	q-axis component of the transient internal emf proportional to the field winding flux linkages
E_d''	[pu]	d-axis component of the sub-transient internal emf proportional to the total flux linkages in the q-axis damper winding and q-axis solid steel rotor body
E_q''	[pu]	q-axis component of the sub-transient internal emf proportional to the total flux linkages in the d-axis damper winding and the field winding
E_{fd}	[pu]	excitation emf proportional to the excitation voltage
f_0	[Hz]	rated frequency of power system (50 Hz in this paper)
f_i	[Hz]	frequency of oscillation corresponding to an eigenvalue
h_1	[s^{-1}]	derivative of water head with respect to time
h	[pu]	water head
I_d, I_q	[pu]	d- and q-axis component of the armature current
K_a	[pu]	gain of exitation system (automatic voltage regulator)
K_p	[pu]	turbine governor parameters: for proportional term
K_i	[pu]	turbine governor parameters: for integral term

K_ω, K_{Pe}	[pu]	gain of power system stabilizer for selecting different input
K_s,	[pu]	gain of power system stabilizer
L	[m]	length of penstock
P_e, P_m	[pu]	electromagnetic active power and mechanical power
Q_g	[pu]	reactive power of generator
T_0, T_1, T_2	[s]	parameters of power system stabilizer
T'_{d0}, T''_{d0}	[s]	open-circuit d-axis transient and sub-transient time constants
T''_{q0}	[s]	open-circuit d-axis sub-transient time constants
T_e	[s]	time constant of water column elasticity, $T_e = L/c$
T_j	[s]	mechanical time constant
T_s	[s]	time constant of surge (in surge tank or gate shaft, etc.)
T_r	[s]	time constant in exitation system (automatic voltage regulator)
T_w	[s]	water starting time constant
T_y	[s]	servo time constant
V_g	[pu]	voltage at the generator terminal
V_{gd}, V_{gq}	[pu]	d- and q-axis component of the voltage at the generator terminal
V_{sd}, V_{sq}	[pu]	d- and q-axis component of the infinite bus voltage
V_s	[pu]	infinite bus voltage
V_1	[pu]	signal between washout and phase compensation block in power system stabilizer
V_{PSS}	[pu]	output signal of power system stabilizer
X_d, X'_d, X''_d	[pu]	d-axis synchronous, transient and sub-transient reactance of generator
X_q, X''_q	[pu]	q-axis synchronous and sub-transient reactance of generator
X_s	[pu]	total reactance of transmission line (between generator and infinite bus)
$X''_{d\Sigma}$, $X''_{q\Sigma}$	[pu]	$X''_{d\Sigma} = X''_d + X_s$; $X''_{q\Sigma} = X''_q + X_s$
y	[pu]	guide vane opening
y_{PI}	[pu]	guide vane opening signal between PI terms and servo
α	[pu]	elasticity coefficient of penstock

δ	[rad]	power (or rotor) angle
φ	[rad]	power factor angle at the generator terminal
ξ_i	/	damping ratio of oscillation corresponding to an eigenvalue
ω	[pu]	angular velocity of the generator
ω_0	[rad/s]	synchronous angular velocity in electrical radians (equals to $2\pi f_0$)
Δ	/	stands for the deviation from the initial value

1. Introduction

Hydropower has played an important role in the operation of electric power systems for a long time. However, new challenges for this relatively mature technology are still emerging. First, the amount of electricity generated by intermittent renewable energy sources has been constantly growing [1, 2]. Hydropower, as the largest global renewable energy source, shoulders a large portion of the work related to regulation and balancing of power systems. Second, the generator size and the complexity of waterway systems in hydropower plants (HPPs) have been increasing. Especially in China [3], dozens of HPPs with at least 1000 MW capacity are being planned, designed, constructed or operated. Third, many large HPPs are located far away from load centers, forming the hydro-dominant power system [4, 5] in China and Sweden. Hence, the demand on the quality of regulation emanating from hydropower units has been increasing. Stable operation of HPPs and their interaction with power systems is of great importance. Especially in recent years, the response rapidity of frequency control is needed [6], and this would enlarge the interaction between hydraulic-mechanical subsystem and electrical subsystem.

Previous research on the stability and dynamic processes of HPPs can be divided into three categories. (1) The first category focuses on the electrical perspective by simplifying the hydraulic and mechanical systems, and this is the standard approach for small signal stability analysis in textbooks [7, 8]. In studies on inter-area mode oscillation [9-12], the hydro turbine model is very simple. (2) The second category is to simplify the electrical sub-system with the first-order swing equation of generating units, such as studies on modeling and transients of the hydraulic-mechanical system [13-19] and the frequency control of HPPs [6, 20-32]. (3) In recent years, studies on coupling of the hydraulic-mechanical-electrical subsystems with relatively detailed models of all three subsystems have been

active. The comprehensive modeling and corresponding simulations of the dynamic processes were conducted in [33-39]. Various controllers were proposed or optimized for enhancing system stability in [40-45]. Eigenvalue analysis on the stability of HPPs were performed in [46-48] based on phase variables a, b, c instead of d, q-components. An eigen-analysis was conducted for the oscillatory instability of a HPP, and influence of the water conduit dynamics was discussed in [49]. The second-order oscillation mode of hydropower systems was studied in [50] based on a linear elastic model and modal analysis. However, there are still limitations in these studies. Most of the previous works only conducted numerical simulations and did not theoretically explain the oscillation mechanism. While in case of works that include theoretical analysis, the hydraulic-mechanical-electrical subsystems is still relatively simple, and only limited factors are discussed. Hence, a fundamental and comprehensive study on the stability of the multi-variable hydropower systems is very important.

This paper aims to conduct a fundamental study on hydraulic-mechanical-electrical coupling mechanism for small signal stability of HPPs. The main focus is on the influence from hydraulic-mechanical factors. For the local mode oscillation [7] in a Single-Machine-Infinite-Bus (SMIB) system, the theoretical eigen-analysis is the core approach and a twelfth-order state matrix is established. A simulation model based on Simulink/SimPowerSystems is built for validation. The common ranges of some standard time constants in hydropower systems are presented in Figure 1, for indicating the interactions among the multiple physical quantities. Time constants regarding the electrical sub-system (generator) are in red, and time constants regarding hydraulic and mechanical sub-systems are in blue. The definitions of the symbols are in Nomenclature. Three principal time constants for water column elasticity (T_e), water inertia (T_w), and servo (T_y) in the hydraulic-mechanical subsystem are the main study objects. They are analyzed under two modes of frequency control (opening feedback and power feedback) without the power system stabilizer (PSS). However, the surge in surge tanks (indicated by T_s) has a relatively slow oscillation and it is excluded in this work. Besides, the influence from the hydraulic-mechanical subsystem on the PSS is investigated.

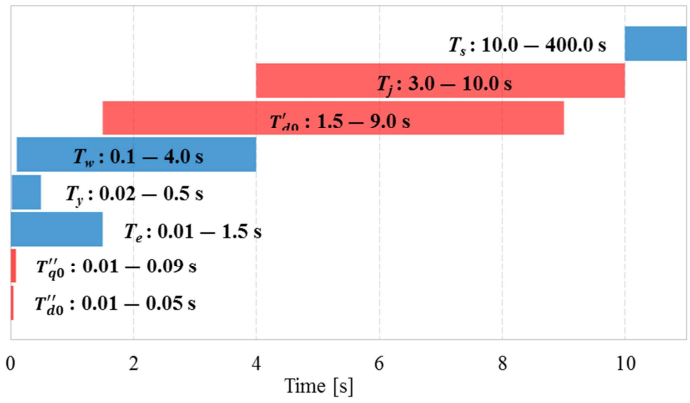

Figure 1. Common ranges of some standard time constants in the hydropower system

The content of this paper is organized as follows. Section 2 describes the models and methods for theoretical analysis and numerical simulation. Section 3 presents the eigen-analysis for exploring the theoretical mechanism and the simulation to support the theoretical analysis. In Section 4, discussions are conducted and the future works are suggested. In Section 5, the main conclusions and significance of this work are summarized.

2. Models and methods

The objective of this study is to propose a SMIB system with an extended model of a hydropower plant. In this section, first, a state matrix of the system is built and the analysis method is briefly introduced. Second, the numerical model based on Simulink/SimPowerSystems and the basic simulation settings are demonstrated. Then, a real case of a Swedish HPP is examined as a case study.

2.1 State matrix and eigen-analysis

The approach of the state space modeling and eigen-analysis on a SMIB system is introduced in detail in [7].

2.1.1 Generator and network

In order to study the SMIB system, the models of the generator and the network are described by the classical fifth-order model [8], as shown in (1) and (2) respectively. Resistance in the systems is ignored. The transformer and

transmission line are simplified as a reactance (X_s).

$$\begin{cases} \dfrac{d\delta}{dt} = (\omega - 1)\,\omega_0 \\ T_j \dfrac{d\omega}{dt} = P_m - P_e \\ T'_{d0} \dfrac{dE'_q}{dt} = E_{fd} - E'_q - I_d (X_d - X'_d) \\ T''_{d0} \dfrac{dE''_q}{dt} = E'_q - E''_q - I_d (X'_d - X''_d) \\ T''_{q0} \dfrac{dE''_d}{dt} = -E''_d + I_q (X_q - X''_q) \end{cases} \tag{1}$$

$$\begin{cases} V_{gd} = V_{sd} - I_q X_s = V_s \sin\delta - I_q X_s \\ V_{gq} = V_{sq} + I_d X_s = V_s \cos\delta + I_d X_s \\ V_{gd} = E''_d + I_q X''_q \\ V_{gq} = E''_q - I_d X''_d \\ V_g^2 = V_{gd}^2 + V_{gq}^2 \\ P_e = I_d V_{gd} + I_q V_{gq} \end{cases} \tag{2}$$

2.1.2 Automatic voltage regulator and power system stabilizer

A standard first-order model [7] of automatic voltage regulator (AVR) is adopted, as described in (3) and Figure 2.

$$T_r \frac{d\Delta E_{fd}}{dt} = -\Delta E_{fd} + K_a \left(-\Delta V_g + \Delta V_{PSS}\right) \tag{3}$$

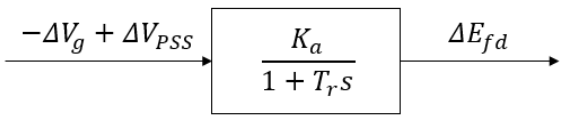

Figure 2. Block diagram of the excitation system

A second-order power system stabilizer model [7] is applied, as described in (4) and Figure 3. In [7], only the input of speed deviation ($\Delta\omega$) is considered while in this study, the input of the deviation of the electromagnetic power (ΔP_e) is also included, for the practical case of the Swedish HPP (Section 2.3).

$$\begin{cases} \dfrac{d\Delta V_1}{dt} = K_s \dfrac{d\Delta I_{PSS}}{dt} - \dfrac{\Delta V_1}{T_0}, \ (\Delta I_{PSS} = K_\omega \Delta\omega - K_{Pe}\Delta P_e) \\ \dfrac{d\Delta V_{PSS}}{dt} = \dfrac{T_1}{T_2} \cdot \dfrac{d\Delta V_1}{dt} + \dfrac{\Delta V_1}{T_2} - \dfrac{\Delta V_{PSS}}{T_2} \end{cases} \tag{4}$$

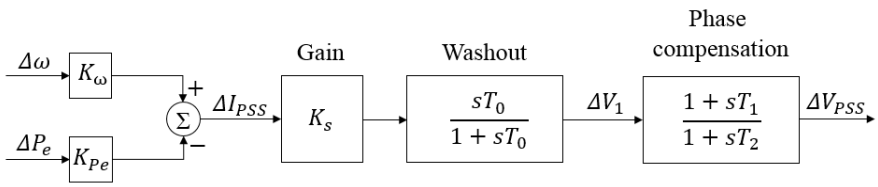

Figure 3. Block diagram of the PSS

2.1.3 Hydro turbine and elastic penstock

A linearized hydro turbine model is applied, by adopting the standard method with six coefficients [7], as shown in (5). The elasticity of the water column [7] is considered, as described in (6), and the frictional loss is ignored here.

$$\text{Turbine characteristic: } \begin{cases} \Delta q = e_{qy}\Delta y + e_{q\omega}\Delta\omega + e_{qh}\Delta h \\ \Delta P_m = e_y \Delta y + e_\omega \Delta\omega + e_h \Delta h \end{cases} \tag{5}$$

$$\text{Elastic water column: } \frac{\Delta h}{\Delta q} = \frac{-T_w s}{1 + \alpha T_e^{\,2} s^2} \tag{6}$$

From (5) and (6), the differential equation (8) can be deduced based on (7).

$$\frac{d\Delta h}{dt} = \Delta h_1 \tag{7}$$

$$\frac{d\Delta h_1}{dt} = \frac{1}{\alpha T_r^{\,2}} \left[-\Delta h - T_w \left(e_{qy} \frac{d\Delta y}{dt} + e_{q\omega} \frac{d\Delta\omega}{dt} + e_{qh} \frac{d\Delta h}{dt} \right) \right] \tag{8}$$

2.1.4 Governor system

For the theoretical analysis, the linear model of the governor system with a proportional–integral (PI) controller with droop and the servo is shown in Figure 4. The nonlinear components with dashed outline are only applied in the simulation model. The equations of frequency control with opening feedback (OF) and power feedback (PF) [16] are

(9) and (10) respectively. It is worth noting that the power feedback signal here is the electromagnetic power, not the mechanical power.

$$\text{Opening feedback: } \left(1+b_pK_p\right)\frac{d\Delta y_{PI}}{dt}+b_pK_i\Delta y_{PI}=-K_p\frac{d\Delta\omega}{dt}-K_i\Delta\omega \tag{9}$$

$$\text{Power feedback: } \frac{d\Delta y_{PI}}{dt}=-b_pK_p\frac{d\Delta P_e}{dt}-b_pK_i\Delta P_e-K_p\frac{d\Delta\omega}{dt}-K_i\Delta\omega \tag{10}$$

$$\text{Servo: } T_y\frac{d\Delta y}{dt}=\Delta y_{PI}-\Delta y \tag{11}$$

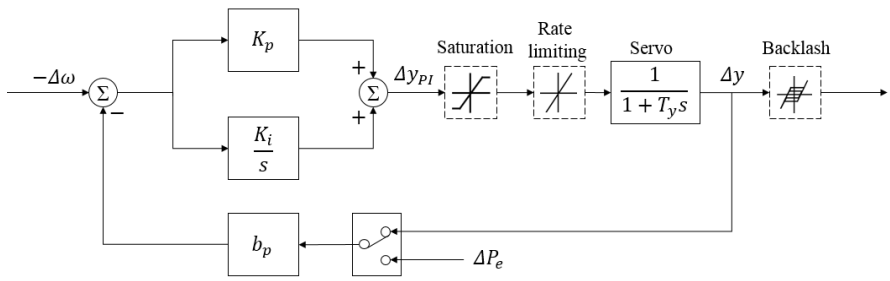

Figure 4. Block diagram of the governor system.

2.1.5 State matrix of the whole system

The free motion of a system can be described by

$$\Delta\dot{x}=A\Delta x. \tag{11}$$

Here, the column vector x means the state vector and the derivative of the state variable with respect to time is $\dot{x}$. A is the state matrix of the system, and it is the core of this paper because the small signal stability of the system can be analyzed by investigating the eigenvalues of the state matrix. There are twelve differential equations for the whole system presented above, i.e. five equations for the generator, one equation for the AVR, two equations for the PSS, two equations for the turbine with the waterway system and two equations for the governor system. Hence, twelve corresponding state variables are applied, as shown in (12).

$$\begin{bmatrix} \Delta\dot{\delta} \\ \Delta\dot{\omega} \\ \Delta\dot{E}'_q \\ \Delta\dot{E}''_q \\ \Delta\dot{E}''_d \\ \Delta\dot{E}_{fd} \\ \Delta\dot{y}_{PI} \\ \Delta\dot{y} \\ \Delta\dot{h}_1 \\ \Delta\dot{h} \\ \Delta\dot{V}_1 \\ \Delta\dot{V}_{PSS} \end{bmatrix} = \begin{bmatrix} 0 & a_{1,2} & 0 & 0 & 0 & 0 & 0 & 0 & 0 & 0 & 0 & 0 \\ a_{2,1} & a_{2,2} & 0 & a_{2,4} & a_{2,5} & 0 & 0 & a_{2,8} & 0 & a_{2,10} & 0 & 0 \\ a_{3,1} & 0 & a_{3,3} & a_{3,4} & 0 & a_{3,6} & 0 & 0 & 0 & 0 & 0 & 0 \\ a_{4,1} & 0 & a_{4,3} & a_{4,4} & 0 & 0 & 0 & 0 & 0 & 0 & 0 & 0 \\ a_{5,1} & 0 & 0 & 0 & a_{5,5} & 0 & 0 & 0 & 0 & 0 & 0 & 0 \\ a_{6,1} & 0 & 0 & a_{6,4} & a_{6,5} & a_{6,6} & 0 & 0 & 0 & 0 & 0 & a_{6,12} \\ a_{7,1} & a_{7,2} & a_{7,3} & a_{7,4} & a_{7,5} & 0 & a_{7,7} & a_{7,8} & 0 & a_{7,10} & 0 & 0 \\ 0 & 0 & 0 & 0 & 0 & 0 & a_{8,7} & a_{8,8} & 0 & 0 & 0 & 0 \\ a_{9,1} & a_{9,2} & 0 & a_{9,4} & a_{9,5} & 0 & a_{9,7} & a_{9,8} & a_{9,9} & a_{9,10} & 0 & 0 \\ 0 & 0 & 0 & 0 & 0 & 0 & 0 & 0 & a_{10,9} & 0 & 0 & 0 \\ a_{11,1} & a_{11,2} & a_{11,3} & a_{11,4} & a_{11,5} & 0 & 0 & a_{11,8} & 0 & a_{11,10} & a_{11,11} & 0 \\ a_{12,1} & a_{12,2} & a_{12,3} & a_{12,4} & a_{12,5} & 0 & 0 & a_{12,8} & 0 & a_{12,10} & a_{12,11} & a_{12,12} \end{bmatrix} \begin{bmatrix} \Delta\delta \\ \Delta\omega \\ \Delta E'_q \\ \Delta E''_q \\ \Delta E''_d \\ \Delta E_{fd} \\ \Delta y_{PI} \\ \Delta y \\ \Delta h_1 \\ \Delta h \\ \Delta V_1 \\ \Delta V_{PSS} \end{bmatrix} \quad (12)$$

Here, all the non-zero elements, $a_{i,j}$, of the state matrix are shown in Appendix. From the state matrix, one can obtain the eigenvalues ($\lambda_i = \alpha_i + j\beta_i$), which are the main indicators of system stability, and the corresponding main participating variables. From an eigenvalue (λ_i), the frequency (f_i) and the damping ratio (ξ_i) of the corresponding oscillation can be obtained [51]:

$$f_i = \frac{\beta_i}{2\pi} \quad (13)$$

$$\xi_i = \frac{-\alpha_i}{\sqrt{\alpha_i^2 + \beta_i^2}} \quad (14)$$

Analyses in the next section involve damping ratios corresponding to different eigenvalues in the system for each case. The smallest damping ratio is selected as the main indicator of the system stability.

2.2 Numerical model and simulation case

In order to validate the theoretical eigen-analysis, time-domain simulation of the system under a three phase fault is conducted. The numerical simulation is implemented in Simulink/SimPowerSystem, and the overall model that contains several subsystems is illustrated in Figure 5. The inputs of reference values are not shown. The signal of rotational speed (ω) is in blue, and the signal of electromagnetic power (P_e) is in red. The numerical model of the

governor is presented in Figure 4, including the nonlinear components with a dashed outline. The rate limitation, backlash and servo are important because they have a decent influence on the response of guide vane opening (GVO) that affects mechanical power of the turbine. The numerical turbine and waterway system model is still linear (Figure 6), corresponding to the theoretical model described by (5) and (6). The numerical models of the AVR and the PSS have the same structure as the theoretical models. The existing blocks "Synchronous Machine" and "Three-Phase Transformer (two windings)" from the SimPowerSystem library are applied. Compared to a standard example "Synchronous Machine" existing in SimPowerSystem, the model built in this study can be regarded as an extension with the PSS added and with more detailed governor, turbine and waterway models.

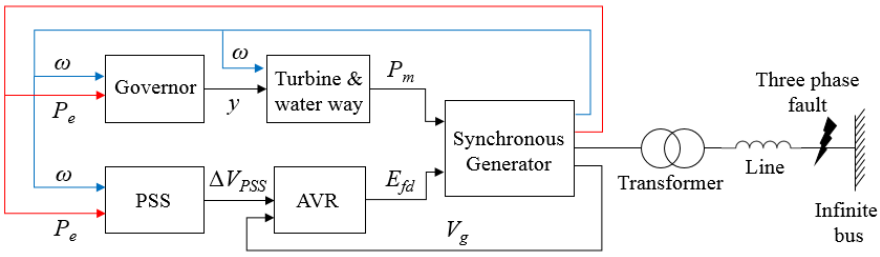

Figure 5. Block diagram of the SMIB system with the extended hydropower plant model

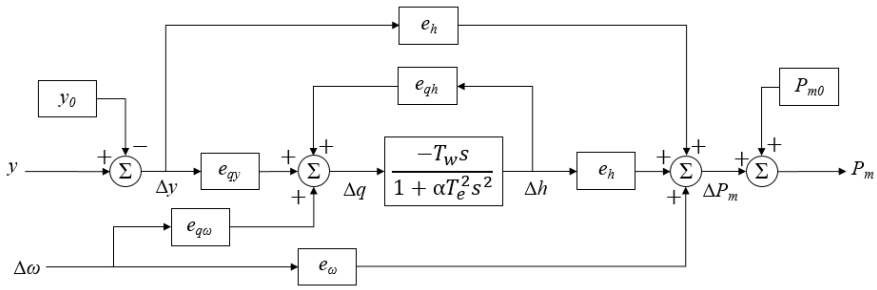

Figure 6. Block diagram of the linear hydro turbine model

The simulation case is a three phase fault that happens on the terminal of infinite bus (in Figure 5) at 1.0 s, and the clearance time is 0.1 s. In the Simulink model, the fault is implemented by inserting a voltage disturbance that is applying a "Three-Phase Programmable Voltage Source" block; another option is to adopt the "Three-Phase Fault" block from the Simulink library, and these two methods are equivalent.

2.3 Study case: a Swedish HPP

The engineering case of this study is a Swedish HPP owned by Vattenfall, the largest hydropower operator in Sweden. The HPP contains four generating units with Francis turbines, and one of the units is taken as the study case. The values of main parameters are shown in Appendix. The values of the generator parameters are estimated from field simulations of standard tests in [52, 53]. Total impedance of the transformer and the transmission line (X_s) is set to 0.3 pu. The tunable operating settings (e.g. settings of turbine governor, AVR, and PSS) of the HPP might be not exactly the same as the values in the practical cases, and the default settings are given in Appendix.

3. Results

In this section, the coupling mechanism of multiple quantities and the influence of three important hydraulic-mechanical factors are analyzed under two modes of frequency control (opening feedback and power feedback) without PSS. Then, the influence from hydraulic-mechanical subsystems on the PSS is investigated. The default parameter settings are in Appendix.

3.1 Water column elasticity (T_e)

Under different conditions of water column elasticity and governor feedback modes, eigenvalues and the corresponding main participating variables of the oscillation modes are shown in Table I, without the engagement of PSS. Three oscillation modes occurred in these conditions, the electro-mechanical mode and the exciter mode are well-known [7], and the water elasticity mode has also been observed in [49]. When power feedback is applied, the interaction between variables is stronger than under opening feedback. Note that a very small value of T_e (e.g. 0.01s) indicates that either the length of waterway is short or the effect of water column elasticity is ignored as in many previous studies.

A more exact analysis is illustrated in Figure 7. The smallest damping ratio (ξ) of all oscillation modes is plotted for each case (one combination of the value of K_p and T_e) under two feedback modes (OF and PF). As shown in Figure 7 (a), when the value of T_e is small (short penstock), the increased response rapidity of the frequency control (indicated by an increase of the K_p value) with OF leads to a smaller damping ratio of the system. On the contrary, when the

value of T_e is larger than a certain value, the system becomes more stable with stronger frequency control. Moreover, the trend is inverted when the governor applies the power feedback; the increased strength of the frequency control stabilizes the system with the small value of T_e. It also corresponds to the relationship between eigenvalues of electro-mechanical mode in Table I under the two feedback modes. Besides, PF generally leads to higher damping ratios than OF.

Table I. Eigenvalues of the system under different conditions of water column elasticity and governor feedback modes.

Mode	No PSS (K_ω =0, K_{Pe} =0)							
	Rigid water column (T_e =0.01 s)				Elastic water column (T_e =1.0 s)			
	Governor with OF		Governor with PF		Governor with OF		Governor with PF	
	λ	Variable	λ	Variable	λ	Variable	λ	Variable
Electro-mechanical	0.0523 ± 8.3022j	Δδ, Δω	-0.4585 ± 7.8138j	Δδ, Δω	-0.1654± 8.4933j	Δδ, Δω	-0.1115 ± 8.7312j	Δδ, Δω
Exciter	-6.1036 ± 8.3635j	$\Delta E_q'$, $\Delta E_q''$, ΔE_{fd}	-6.1826 ± 8.3576j	$\Delta E_q'$, $\Delta E_q''$, ΔE_{fd}	-6.0891± 8.3883j	$\Delta E_q'$, $\Delta E_q''$, ΔE_{fd}	-6.0604 ± 8.3982j	$\Delta E_q'$, $\Delta E_q''$, ΔE_{fd}
Water elasticity	/	/	/	/	-0.9635± 1.4875j	Δh_1, Δh	-0.5807 ± 1.3384j	Δh_1, Δh, $\Delta\delta$, Δy_{PI}, Δy

1. The corresponding main participation variables of the oscillation mode are presented in the column "Variable".
2. The "OF" and "PF" stand for opening feedback and power feedback respectively.
3. Other parameter settings adopt the default values in Appendix.

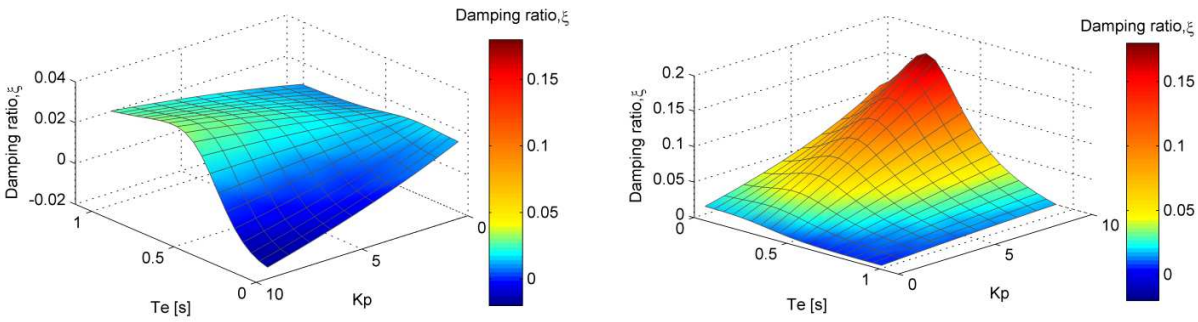

(a) **(b)**

Figure 7. The smallest damping ratio (ξ) under different cases and feedback modes. (a) OF; (b) PF.

The observations above are further validated by time domain simulations. As shown in Figure 8, the blue line shows a medium situation under the original value of T_e without frequency control while the black line represents a higher

damping ratio, i.e. oscillation is dampened within 7 s; the red line represents oscillation under a less stable condition. The simulation results of these three sets of parameters fit the damping ratio well (the result validates the cases in Figure 7). In short, the impact of water column elasticity is important and it differs from the feedback mode of the frequency control.

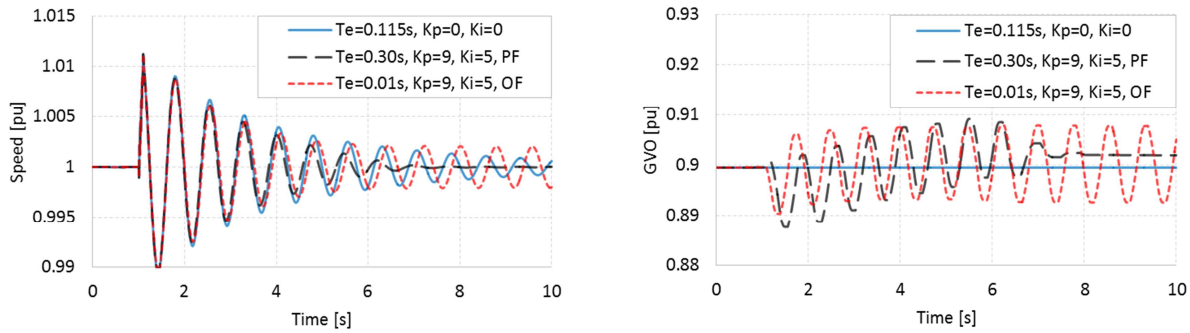

(a) **(b)**

Figure 8. Simulation of the process after the three phase fault: (a) Rotational speed (b) Turbine GVO.

3.2 Mechanical components in governor system (T_y)

The mechanical components (servo, backlash, rate limiter, etc.) in the governor system determine the rapidity of the GVO response. In the state matrix, these components are simplified and represented by the servo time constant (T_y). Figure 9 shows the damping ratio under different values of servo time constant (T_y) in various conditions. A small value of T_y leads to a quicker response of GVO, and brings clearer influence on system stability. The influence of T_y is more obvious when K_p is larger. A time domain simulation for OF in Figure 10 (a) demonstrates the influence and it corresponds to the result in Figure 9 (b).

Besides, the linear theoretical model can result in negative damping ratios (Table I, Figure 7 and Figure 9). However, the oscillations are not divergent in the simulations. The reason is the added damping by the nonlinear components in the numerical model, mainly from the rate limiter, as shown in Figure 10 (b). While detailed investigation of various nonlinear factors in the governor is out of the scope of this work, it could be an interesting future work.

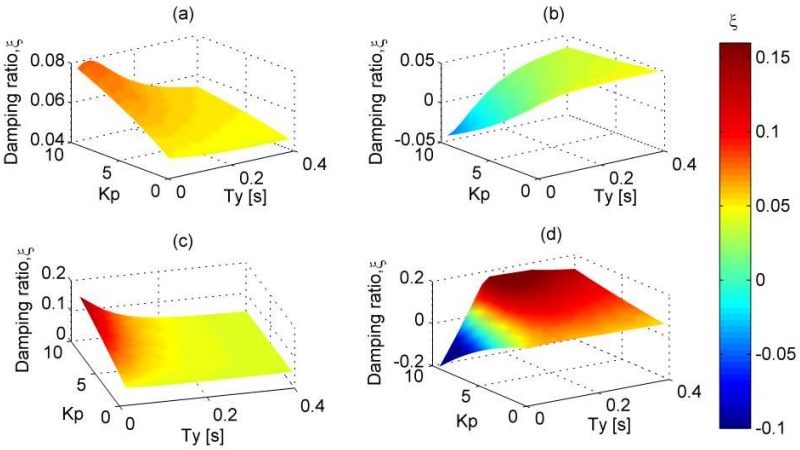

Figure 9. The smallest damping ratio (ξ) under different cases and feedback modes. (a) OF, T_e = 1.0; (b) OF, T_e = 0.01; (c) PF, T_e = 1.0; (d) PF, T_e = 0.01.

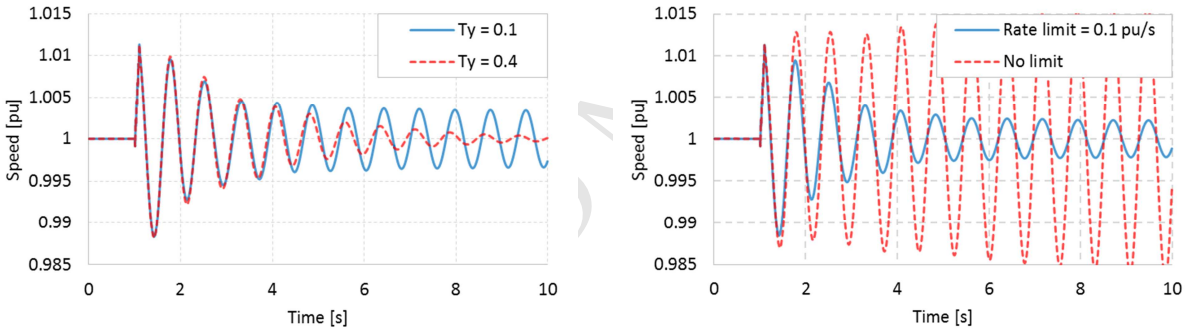

(a) **(b)**

Figure 10. Simulation of rotational speed after the three phase fault. (a) cases under different values of T_y; (b) cases with and without rate limiter

3.3 Water inertia (T_w)

The water inertia, represented by the water starting time constant (T_w), is normally regarded as adverse to system stability, especially in islanding operating conditions [24, 25]. While for the SMIB system, the influence of water inertia is not monotonic, as shown in Figure 11 and Figure 12. It is shown that the effect of water inertia differs from that of water column elasticity. Figure 12 shows that a larger value of T_w leads to smaller damping ratio when the

value of water column elasticity (T_e) is around 0.4 and this can be observed in Figure 11 (a). However, the increase of T_w results in slightly more stable cases when the value of T_e is large or small, as demonstrated in Figure 12 and Figure 11 (b). When the governor adopts the power feedback, the system is more stable under larger water inertia in this case, and this is validated by time domain simulations: the result in Figure 13 validates the cases in Figure 11 (d).

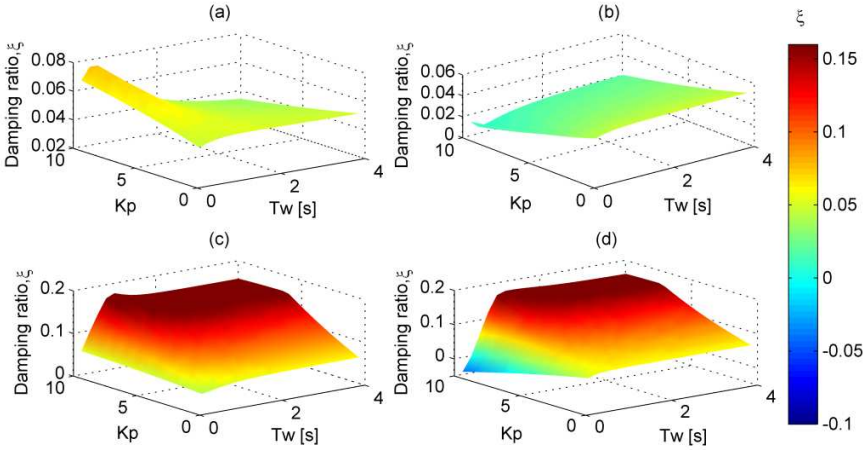

Figure 11. The smallest damping ratio (ξ) under different cases and feedback modes. (a) OF, T_e = 0.4; (b) OF, T_e = 0.01; (c) PF, T_e = 0.4; (d) PF, T_e = 0.01.

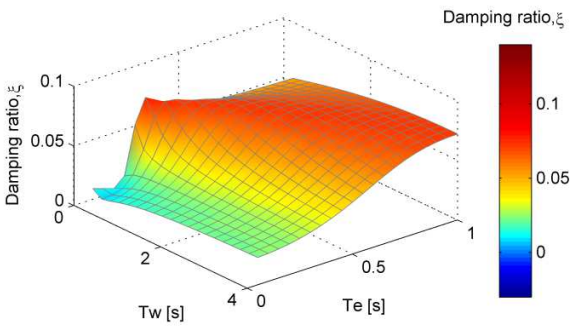

Figure 12. The smallest damping ratio (ξ) of all the oscillation modes under different cases (under OF).

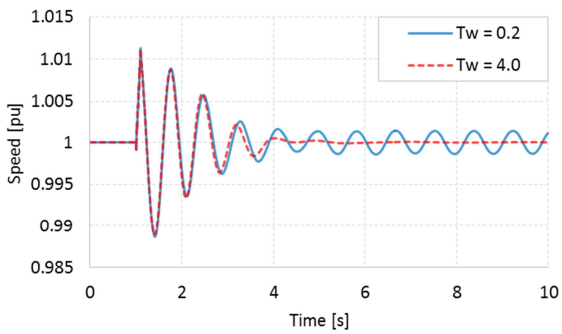

Figure 13. Simulated rotational speed after the three phase fault under different values of T_w (under PF).

3.4 Influence on tuning of PSS

In this subsection, the influence of hydraulic-mechanical factors on tuning of the PSS is investigated. The damping effects of a PSS with different settings of parameters K_s and T_2 under various conditions are shown in Figure 14 and Figure 15 respectively. First, the optimal parameters values vary with different types of feedback. More exactly, for achieving the largest damping ratio, the K_s value differs in four cases, shown in Figure 14 (a) - (d); this also applies to the value of T_2, as presented in Figure 15 (The varying ranges of T_2 are different for two types of PSS). Note that the optimal values of K_s and T_2 change with different types of PSS. Meanwhile, the water column elasticity also affects the tuning. Second, the stability margin changes considerably under various conditions. The frequency control with the power feedback generally leads to a higher damping ratio, and this is validated by the time domain simulations in Figure 16: the PSS adopts speed input and the gain K_s is set to 4.0, and the result validates the cases in Figure 14 (a) and (c). It can be observed that there is still room for optimizing the parameter and performance of the PSS by considering the effect of the hydraulic-mechanical factors. It is worth noting that the analysis only aims to demonstrate that the performance of PSS can be considerably affected, and the detailed parameter tuning is out of the scope.

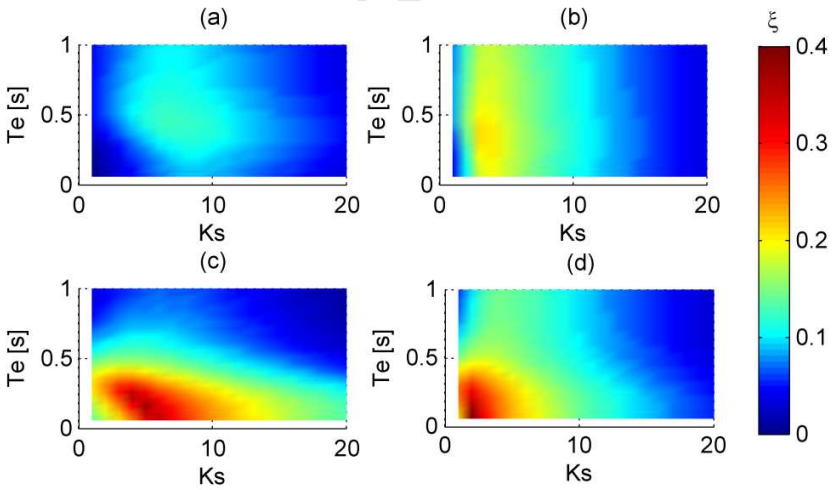

Figure 14. The smallest damping ratio (ξ) under different cases: (a) OF, speed input in PSS; (b) OF, power input in PSS; (c) PF, speed input in PSS; (d)PF, power input in PSS.

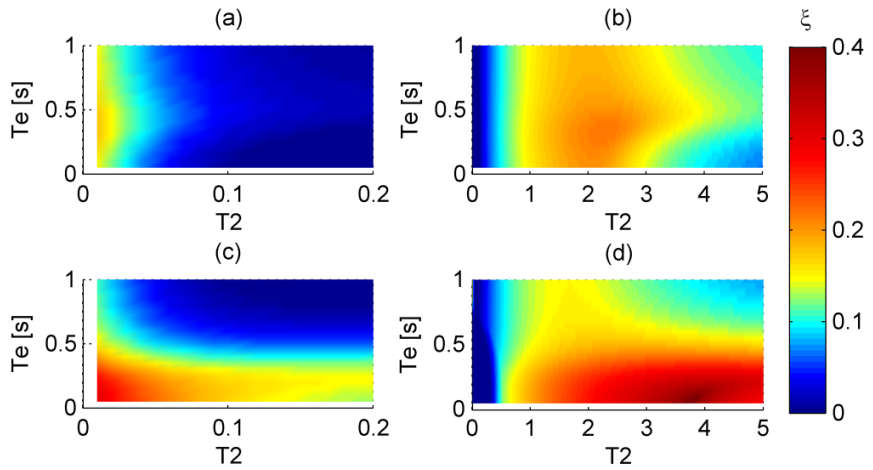

Figure 15. The smallest damping ratio (ξ) under different cases: (a) OF, speed input in PSS; (b) OF, power input in PSS; (c) PF, speed input in PSS; (d)PF, power input in PSS.

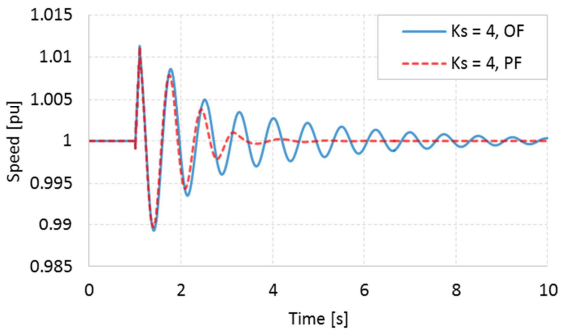

Figure 16. Simulated rotational speed after the three phase fault under different feedback modes of governor

4. Discussion

A key point of this study is whether the governor response is quick enough to trigger an obvious coupling effect between the hydraulic-mechanical subsystem and the electrical subsystem. Previously the effect of turbine governor has often been ignored in the small signal stability analysis [7]; however in recent years, the rapidity of primary frequency control has been demanded in order to ensure quick response, according to requirements of TSOs [6]. For example, in a huge hydropower plant in China, values of the governor parameters K_p and K_i are in practice set to 9.0 and 8.0 respectively, leading to very fast GVO response. Hence, the value of K_p is also set to 9.0 in this work.

Meanwhile, the quick GVO response after a three phase fault can also be found in simulation cases in previous research [40, 41, 44]. Especially in [44], the fast GVO change process is clearly demonstrated in a field experiment. What's more, in this work, practical nonlinear components (servo, backlash, rate limit) are included and the values are set according to real engineering cases. All these factors tend to slow the governor response. In short, the concern on the rapidity of governor response is fully considered in this study, and the cases are practical and even stricter than previous works.

Besides, this work could be extended in the following aspects. (1) An ideal future work is a more refined simulation study and physical experiments on the coupling mechanism of the hydraulic-mechanical-electrical system. It is necessary to conduct a specific study on the influence from turbine characteristics, especially for pumped storage HPPs in which stability of operations is relatively more problematic [54]. (2) A specific study on parameter tuning of AVR and PSS, by considering the influences of the hydraulic-mechanical system, could be meaningful. (3) An ultimate goal is to study the stability of systems with multiple hydro units and the inter-area mode oscillations.

5. Conclusions

In this work, a fundamental study on the hydraulic-mechanical-electrical coupling mechanism is conducted for small signal stability of HPPs. A twelfth-order state matrix is established and a simulation model based on Simulink/SimPowerSystems is introduced. New insights are found and the conclusions are as follows.

(1) The influence from the hydraulic-mechanical subsystem on the electrical subsystem is analyzed, and interactions between multiple physical variables are demonstrated. The effect of turbine governor actions is no longer ignorable for the local mode oscillation due to the increasing rapidity of frequency control nowadays. (2) Previous studies have mainly investigated the influencing factor (e.g. water inertia) individually, without much consideration of the coupling effect between diverse variables under different conditions of governor control. In this work, based on comprehensive modeling and analysis, it is shown that influences from single factors are not monotonic and depend on the interactions with other factors. Opening feedback and power feedback mode of frequency control lead to different performances, and their impacts mainly differ according to the water column elasticity. The consideration of

water column elasticity (T_e) is of great importance, and it significantly affects other factors. The mechanical component in the governor (T_y), which determines the rapidity of GVO response, also has a non-ignorable effect. The influence of water inertia (T_w), which is normally regarded as adverse to the system stability, varies in different conditions, and it can contribute to the system stability in certain cases. (3) There is still room for parameter tuning of controllers (e.g. turbine governor, AVR, and PSS) by considering the influence of the hydraulic-mechanical factors.

A core contribution of this work is the state matrix. All elements in the state matrix are demonstrated clearly for other scholars to conveniently conduct further investigations. It could be an efficient approach for further research and engineering applications, such as controller parameter tunings (e.g. PSS, governor and AVR) for different HPPs with various conditions of the hydraulic-mechanical system. This study also supplies new insights and lays a good foundation for research on systems with multiple hydro units and the inter-area mode oscillation.

Acknowledgements

The research presented was carried out as a part of "Swedish Hydropower Centre - SVC". SVC has been established by the Swedish Energy Agency, Elforsk and Svenska Kraftnät together with Luleå University of Technology, KTH Royal Institute of Technology, Chalmers University of Technology and Uppsala University (www.svc.nu). The authors also thank the China Scholarship Council (CSC), StandUp for Energy, and the support from the National Natural Science Foundation of China under Grant No. 51379158.

Appendix

A. Elements of the state matrix:

$$a_{1,2}=\omega_0=2\pi f_0,\ a_{2,1}=-\frac{K_1}{T_j},\ a_{2,2}=\frac{e_\omega}{T_j},\ a_{2,4}=-\frac{K_2}{T_j},\ a_{2,5}=-\frac{K_3}{T_j},\ a_{2,8}=\frac{e_y}{T_j},\ a_{2,10}=\frac{e_h}{T_j},$$

$$a_{3,1}=-\frac{K_4\left(X_d-X_d'\right)}{T_{d0}'},\ a_{3,3}=-\frac{1}{T_{d0}'},\ a_{3,4}=-\frac{K_5\left(X_d-X_d'\right)}{T_{d0}'},\ a_{3,6}=\frac{1}{T_{d0}'},\ a_{4,1}=-\frac{K_4\left(X_d'-X_d''\right)}{T_{d0}''},\ a_{4,3}=\frac{1}{T_{d0}''},$$

$$a_{4,4}=-\frac{K_5X_d'-K_5X_d''+1}{T_{d0}''},\ a_{5,1}=\frac{K_6\left(X_q-X_q''\right)}{T_{q0}''},\ a_{5,5}=\frac{K_7X_q-K_7X_q''-1}{T_{q0}''},\ a_{6,1}=-\frac{K_aK_8}{T_r},\ a_{6,4}=-\frac{K_aK_9}{T_r},$$

$$a_{6,5}=-\frac{K_aK_{10}}{T_r},\ a_{6,6}=-\frac{1}{T_r},\ a_{6,12}=\frac{K_a}{T_r},\ a_{8,7}=\frac{1}{T_y},\ a_{8,8}=-\frac{1}{T_y},\ a_{9,1}=-\frac{T_we_{q\omega}a_{2,1}}{\alpha T_e^2},\ a_{9,2}=-\frac{T_we_{q\omega}a_{2,2}}{\alpha T_e^2},$$

$$a_{9,4}=-\frac{T_we_{q\omega}a_{2,4}}{\alpha T_e^2},\ a_{9,5}=-\frac{T_we_{q\omega}a_{2,5}}{\alpha T_e^2},\ a_{9,7}=-\frac{T_we_{qy}a_{8,7}}{\alpha T_e^2},\ a_{9,8}=\frac{-T_we_{q\omega}a_{2,8}-T_we_{qy}a_{8,8}}{\alpha T_e^2},\ a_{9,9}=-\frac{T_we_{qh}}{\alpha T_e^2},$$

$$a_{9,10}=\frac{-1-T_we_{q\omega}a_{2,10}}{\alpha T_e^2},\ a_{10,9}=1,\ a_{11,1}=K_sK_\omega a_{2,1}-K_sK_{Pe}K_2a_{4,1}-K_sK_{Pe}K_3a_{5,1},$$

$$a_{11,2}=K_sK_\omega a_{2,2}-K_sK_{Pe}K_1a_{1,2},\ a_{11,3}=-K_sK_{Pe}K_2a_{4,3},\ a_{11,4}=K_sK_\omega a_{2,4}-K_sK_{Pe}K_2a_{4,4},$$

$$a_{11,5}=K_sK_\omega a_{2,5}-K_sK_{Pe}K_3a_{5,5},\ a_{11,8}=K_sK_\omega a_{2,8},\ a_{11,10}=K_sK_\omega a_{2,10},\ a_{11,11}=-\frac{1}{T_0},\ a_{12,1}=\frac{T_1}{T_2}a_{11,1},$$

$$a_{12,2}=\frac{T_1}{T_2}a_{11,2},\ a_{12,3}=\frac{T_1}{T_2}a_{11,3},\ a_{12,4}=\frac{T_1}{T_2}a_{11,4},\ a_{12,5}=\frac{T_1}{T_2}a_{11,5},\ a_{12,8}=\frac{T_1}{T_2}a_{11,8},\ a_{12,10}=\frac{T_1}{T_2}a_{11,10},$$

$$a_{12,11}=\frac{T_1}{T_2}a_{11,11}+\frac{1}{T_2},\ a_{12,12}=-\frac{1}{T_2}.$$

For opening feedback:

$$a_{(OF)7,1}=-\frac{K_pa_{2,1}}{1+b_pK_p},\ a_{(OF)7,2}=\frac{-K_pa_{2,2}-K_i}{1+b_pK_p},\ a_{(OF)7,3}=0,\ a_{(OF)7,4}=-\frac{K_pa_{2,4}}{1+b_pK_p},\ a_{(OF)7,5}=-\frac{K_pa_{2,5}}{1+b_pK_p},$$

$$a_{(OF)7,7}=-\frac{b_pK_i}{1+b_pK_p},\ a_{(OF)7,8}=\frac{-K_pa_{2,8}}{1+b_pK_p},\ a_{(OF)7,10}=\frac{-K_pa_{2,10}}{1+b_pK_p};$$

For power feedback:

$$a_{(PF)7,1}=-b_pK_iK_1-b_pK_pK_3a_{5,1}-b_pK_pK_2a_{4,1}-K_pa_{2,1},\ a_{(PF)7,2}=-b_pK_iK_1a_{1,2}-K_pa_{2,2}-K_i,$$

$$a_{(PF)7,3}=-b_pK_pK_2a_{4,3},\ a_{(PF)7,4}=-b_pK_iK_2-b_pK_pK_2a_{4,4}-K_pa_{2,4},$$

$$a_{(PF)7,5}=-b_pK_iK_3-b_pK_pK_3a_{5,5}-K_pa_{2,5},\ a_{(PF)7,7}=0,\ a_{(PF)7,8}=-K_pa_{2,8},\ a_{(PF)7,10}=-K_pa_{2,10}.$$

Here, $K_1 - K_{10}$ are:

$$\begin{cases} P_e = E''_d I_d + E''_q I_q + I_d I_q \left(X''_{q\Sigma} - X''_{d\Sigma} \right) \\ \Delta P_e = \dfrac{\partial P_e}{\partial \delta} \Delta\delta + \dfrac{\partial P_e}{\partial E''_q} \Delta E''_q + \dfrac{\partial P_e}{\partial E''_d} \Delta E''_d = K_1 \Delta\delta + K_2 \Delta E''_q + K_3 \Delta E''_d \end{cases} \tag{A-1}$$

$$I_d = \frac{E''_q - V_s \cos\delta}{X''_{d\Sigma}}; \Delta I_d = \frac{\partial I_d}{\partial \delta} \Delta\delta + \frac{\partial I_d}{\partial E''_q} \Delta E''_q = K_4 \Delta\delta + K_5 \Delta E''_q \tag{A-2}$$

$$I_q = \frac{V_s \sin\delta - E''_d}{X''_{q\Sigma}}; \Delta I_q = \frac{\partial I_q}{\partial \delta} \Delta\delta + \frac{\partial I_q}{\partial E''_d} \Delta E''_d = K_6 \Delta\delta + K_7 \Delta E''_d \tag{A-3}$$

$$\begin{cases} V_g = \sqrt{\left(\dfrac{X_s E''_d + X''_q V_s \sin\delta}{X''_{q\Sigma}} \right)^2 + \left(\dfrac{X_s E''_q + X''_d V_s \cos\delta}{X''_{d\Sigma}} \right)^2} \\ \Delta V_g = \dfrac{\partial V_g}{\partial \delta} \Delta\delta + \dfrac{\partial V_g}{\partial E''_q} \Delta E''_q + \dfrac{\partial V_g}{\partial E''_d} \Delta E''_d = K_8 \Delta\delta + K_9 \Delta E''_q + K_{10} \Delta E''_d \end{cases} \tag{A-4}$$

$$K_1 = \frac{E''_d V_s \sin\delta}{X''_{d\Sigma}} + \frac{E''_q V_s \cos\delta}{X''_{q\Sigma}} + \frac{\left(X''_{q\Sigma} - X''_{d\Sigma} \right) \left(E''_q V_s \cos\delta - V_s^2 \cos 2\delta + E''_d V_s \sin\delta \right)}{X''_{d\Sigma} X''_{q\Sigma}},$$

$$K_2 = \frac{E''_d}{X''_{d\Sigma}} + \frac{V_s \sin\delta - E''_d}{X''_{q\Sigma}} + \frac{\left(X''_{q\Sigma} - X''_{d\Sigma} \right) \left(V_s \sin\delta - E''_d \right)}{X''_{d\Sigma} X''_{q\Sigma}},$$

$$K_3 = \frac{E''_q - V_s \cos\delta}{X''_{d\Sigma}} - \frac{E''_q}{X''_{q\Sigma}} + \frac{\left(X''_{q\Sigma} - X''_{d\Sigma} \right) \left(V_s \cos\delta - E''_q \right)}{X''_{d\Sigma} X''_{q\Sigma}}, K_4 = \frac{V_s \sin\delta}{X''_{d\Sigma}}, K_5 = \frac{1}{X''_{d\Sigma}}, K_6 = \frac{V_s \cos\delta}{X''_{q\Sigma}},$$

$$K_7 = -\frac{1}{X''_{q\Sigma}}, K_8 = \frac{V_{gd} V_s \cos\delta X''_q}{V_g X''_{q\Sigma}} - \frac{V_{gq} V_s \sin\delta X''_d}{V_g X''_{d\Sigma}}, K_9 = \frac{V_{gq} x_s}{V_g X''_{d\Sigma}}, K_{10} = \frac{V_{gd} x_s}{V_g X''_{q\Sigma}}.$$

The values of the state variables in the coefficients $K_1 - K_{10}$ are initial steady-state values.

B. Parameter values of the HPP

Generator: the nominal apparent power is 206 MVA, and the line-to-line voltage is 21 kV.

X_d =0.768, X'_d =0.249, X''_d=0.187, X_q =0.512, X''_q=0.189, T'_{d0} =7.880, T''_{d0} =0.049, T''_{q0} =0.0283, T_j=7.0 s;

Transformer and transmission line: X_s =0.30;

Turbine characteristic (for a normal operating point): e_{qy} =0.66, $e_{q\omega}$ =0.1, e_{qh} =0.47, e_y =0.5, e_ω =-0.96, e_h =1.45;

Penstock: T_w =1.34 s (calculated under the rated condition: discharge is 275.0 m^3/s and water head is 73.0 m), α=0.33, T_e =0.115 s (length of the penstock is 115 m).

C. Operating settings of the HPP

Initial steady-state condition: P_e =0.90 pu, $cos\varphi$ =0.90 (Q_g =0.436), V_s =1.00 pu;

Turbine governor (for both two feedback modes): b_p =0.04, K_p =9.0, K_i =5.0, T_y =0.2 s, Backlash=0.001 pu, Limiting rate=0.1 pu/s;

AVR: T_r =0.05, K_a =100, the regulator output limit is ±2.0 pu;

PSS (speed input): K_ω =1, K_{Pe} =0, K_s =9.5, T_0 =1.4, T_1 =0.154, T_2 =0.033;

PSS (power input): K_ω =0, K_{Pe} =1, K_s =2.5, T_0 =1.4, T_1 =0.154, T_2 =3.0.

References

[1] C. Mitchell, Momentum is increasing towards a flexible electricity system based on renewables, Nature Energy, 1 (2016) 15030.

[2] T. Rintamäki, A.S. Siddiqui, A. Salo, How much is enough? Optimal support payments in a renewable-rich power system, Energy, 117 (2016) 300-313.

[3] X. Chang, X. Liu, W. Zhou, Hydropower in China at present and its further development, Energy, 35 (2010) 4400-4406.

[4] H. Zhou, Y. Su, Y. Chen, Q. Ma, W. Mo, The China Southern Power Grid: Solutions to Operation Risks and Planning Challenges, IEEE Power and Energy Magazine, 14 (2016) 72-78.

[5] J. Shen, C. Cheng, X. Cheng, J.R. Lund, Coordinated operations of large-scale UHVDC hydropower and conventional hydro energies about regional power grid, Energy, 95 (2016) 433-446.

[6] W. Yang, J. Yang, W. Guo, P. Norrlund, Response time for primary frequency control of hydroelectric generating unit, International Journal of Electrical Power & Energy Systems, 74 (2016) 16-24.

[7] P. Kundur, N.J. Balu, M.G. Lauby, Power system stability and control, McGraw-hill New York, 1994.

[8] J. Machowski, J. Bialek, J. Bumby, Power system dynamics: stability and control, John Wiley & Sons, 2011.

[9] D. Rimorov, I. Kamwa, G. Joós, Quasi-Steady-State Approach for Analysis of Frequency Oscillations and Damping Controller Design, IEEE Transactions on Power Systems, 31 (2016) 3212-3220.

[10] W. Tan, Unified tuning of PID load frequency controller for power systems via IMC, IEEE Transactions on power systems, 25 (2010) 341-350.

[11] S.A.N. Sarmadi, V. Venkatasubramanian, Inter-Area Resonance in Power Systems From Forced Oscillations, IEEE Transactions on Power Systems, 31 (2016) 378-386.

[12] L. Jiang, W. Yao, Q.H. Wu, J.Y. Wen, S.J. Cheng, Delay-dependent stability for load frequency control with constant and time-varying delays, IEEE Transactions on Power systems, 27 (2012) 932-941.

[13] F. Demello, R. Koessler, J. Agee, P. Anderson, J. Doudna, J. Fish, P. Hamm, P. Kundur, D. Lee, G. Rogers, Hydraulic-turbine and turbine control-models for system dynamic studies, IEEE Transactions on Power Systems, 7 (1992) 167-179.

[14] G.A. Aggidis, A. Židonis, Hydro turbine prototype testing and generation of performance curves: Fully automated approach, Renewable Energy, 71 (2014) 433–441.

[15] H. Fang, L. Chen, N. Dlakavu, Z. Shen, Basic modeling and simulation tool for analysis of hydraulic transients in hydroelectric power plants, IEEE Transactions on Energy Conversion, 23 (2008) 834-841.

[16] W. Yang, J. Yang, W. Guo, W. Zeng, C. Wang, L. Saarinen, P. Norrlund, A Mathematical Model and Its Application for Hydro Power Units under Different Operating Conditions, Energies, 8 (2015) 10260-10275.

[17] D.R. Giosio, A.D. Henderson, J.M. Walker, P.A. Brandner, Physics Based Hydraulic Turbine Model for System Dynamics Studies, IEEE Transactions on Power Systems, (2016).

[18] W. Guo, J. Yang, M. Wang, X. Lai, Nonlinear modeling and stability analysis of hydro-turbine governing system with sloping ceiling tailrace tunnel under load disturbance, Energy Conversion and Management, 106 (2015) 127-138.

[19] H. Li, D. Chen, X. Zhang, Y. Wu, Dynamic Analysis and Modelling of a Francis Hydro-energy Generation System in the Load Rejection Transient, IET Renewable Power Generation, (2016).

[20] J.I. Pérez-Díaz, J.I. Sarasúa, J.R. Wilhelmi, Contribution of a hydraulic short-circuit pumped-storage power plant to the load–frequency regulation of an isolated power system, International Journal of Electrical Power & Energy Systems, 62 (2014) 199-211.

[21] G. Martínez-Lucas, J.I. Sarasúa, J.Á. Sánchez-Fernández, J.R. Wilhelmi, Frequency control support of a wind-

solar isolated system by a hydropower plant with long tail-race tunnel, Renewable Energy, 90 (2016) 362-376.

[22] G. Martínez-Lucas, J.I. Sarasúa, J.Á. Sánchez-Fernández, J.R. Wilhelmi, Power-frequency control of hydropower plants with long penstocks in isolated systems with wind generation, Renewable Energy, 83 (2015) 245-255.

[23] H.V. Pico, J.D. McCalley, A. Angel, R. Leon, N.J. Castrillon, Analysis of Very Low Frequency Oscillations in Hydro-Dominant Power Systems Using Multi-Unit Modeling, IEEE Transactions on Power Systems, 27 (2012) 1906-1915.

[24] W. Yang, J. Yang, W. Guo, P. Norrlund, Frequency Stability of Isolated Hydropower Plant with Surge Tank Under Different Turbine Control Modes, Electric Power Components and Systems, 43 (2015) 1707-1716.

[25] W. Guo, J. Yang, W. Yang, J. Chen, Y. Teng, Regulation quality for frequency response of turbine regulating system of isolated hydroelectric power plant with surge tank, International Journal of Electrical Power & Energy Systems, 73 (2015) 528-538.

[26] H.N.V. Pico, D.C. Aliprantis, J.D. McCalley, N. Elia, N.J. Castrillon, Analysis of hydro-coupled power plants and design of robust control to damp oscillatory modes, IEEE Transactions on Power Systems, 30 (2015) 632-643.

[27] K. Vereide, B. Svingen, T. Nielsen, L. Lia, The Effect of Surge Tank Throttling on Governor Stability, Power Control, and Hydraulic Transients in Hydropower Plants, IEEE Transactions on Energy Conversion, (2016).

[28] H. Li, D. Chen, H. Zhang, C. Wu, X. Wang, Hamiltonian analysis of a hydro-energy generation system in the transient of sudden load increasing, Applied Energy, 185 (2017) 244-253.

[29] X. Yu, J. Zhang, C. Fan, S. Chen, Stability analysis of governor-turbine-hydraulic system by state space method and graph theory, Energy, 114 (2016) 613-622.

[30] X. Yuan, Z. Chen, Y. Yuan, Y. Huang, Design of fuzzy sliding mode controller for hydraulic turbine regulating system via input state feedback linearization method, Energy, 93 (2015) 173-187.

[31] N. Kishor, R. Saini, S. Singh, A review on hydropower plant models and control, Renewable and Sustainable Energy Reviews, 11 (2007) 776-796.

[32] W. Yang, P. Norrlund, L. Saarinen, J. Yang, W. Guo, W. Zeng, Wear and tear on hydro power turbines–Influence from primary frequency control, Renewable Energy, 87 (2016) 88-95.

[33] C. Nicolet, B. Greiveldinger, J.-J. Hérou, B. Kawkabani, P. Allenbach, J.-J. Simond, F. Avellan, High-order modeling of hydraulic power plant in islanded power network, IEEE Transactions on Power Systems, 22 (2007)

1870-1880.

[34] G. Zhao, Study on the United Transient Process for Hydraulic, Mechanical and Power System, in: Department of Water Conservancy and Hydropower Engineering, Wuhan University, 2004.

[35] W. Li, L. Vanfretti, Y. Chompoobutrgool, Development and implementation of hydro turbine and governor models in a free and open source software package, Simulation Modelling Practice and Theory, 24 (2012) 84-102.

[36] A. Padoan, B. Kawkabani, A. Schwery, C. Ramirez, C. Nicolet, J.-J. Simond, F. Avellan, Dynamical behavior comparison between variable speed and synchronous machines with pss, IEEE Transactions on Power Systems, 25 (2010) 1555-1565.

[37] J.W. Tsotie, R. Wamkeue, Advanced-model of synchronous generator for hydropower plants numerical simulations, Electric Power Systems Research, (2016).

[38] J. Liang, X. Yuan, Y. Yuan, Z. Chen, Y. Li, Nonlinear dynamic analysis and robust controller design for Francis hydraulic turbine regulating system with a straight-tube surge tank, Mechanical Systems and Signal Processing, 85 (2017) 927-946.

[39] J.A.S. Sena, M.C.P. Fonseca, I.F. Di Paolo, W. Barra, J.A.L. Barreiros, C.T. Costa, F.G. Nogueira, An object-oriented framework applied to the study of electromechanical oscillations at Tucuruí hydroelectric power plant, Electric Power Systems Research, 81 (2011) 2081-2087.

[40] O. Akhrif, F.A. Okou, L.A. Dessaint, R. Champagne, Application of a multivariable feedback linearization scheme for rotor angle stability and voltage regulation of power systems, IEEE Transactions on Power Systems, 14 (1999) 620-628.

[41] D.M. Dobrijevic, M.V. Jankovic, An approach to the damping of local modes of oscillations resulting from large hydraulic transients, IEEE Transactions on Energy Conversion, 14 (1999) 754-759.

[42] Q. Lu, Y. Sun, Y. Sun, F.F. Wu, Y. Ni, A. Yokoyama, M. Goto, H. Konishi, Nonlinear decentralized robust governor control for hydroturbine-generator sets in multi-machine power systems, International Journal of Electrical Power & Energy Systems, 26 (2004) 333-339.

[43] M.J. Jin, W. Hu, F. Liu, S.W. Mei, Q. Lu, Nonlinear co-ordinated control of excitation and governor for hydraulic power plants, IEE Proceedings-Generation, Transmission and Distribution, 152 (2005) 544-548.

[44] S. Mei, X. Gui, C. Shen, Q. Lu, Dynamic extending nonlinear H∞ control and its application to hydraulic turbine governor, Science in China Series E: Technological Sciences, 50 (2007) 618-635.

[45] M. Alizadeh Bidgoli, S.M.T. Bathaee, Full-state Variables Control of a Grid-connected Pumped Storage Power Plant Using Non-linear Controllers, Electric Power Components and Systems, 43 (2015) 260-270.

[46] P.C.O. Silva, B. Kawkabani, S. Alligné, C. Nicolet, J.J. Simond, F. Avellan, Stability study of a complete hydroelectric production site by eigenvalues analysis method based on phase variables, in: Electrical Machines (ICEM), 2010 XIX International Conference on, IEEE, 2010, pp. 1-6.

[47] P.C.O. Silva, S. Alligné, P. Allenbach, C. Nicolet, B. Kawkabani, A fully modular tool for small-signal stability analysis of hydroelectric systems, in: Electrical Machines (ICEM), 2014 International Conference on, IEEE, 2014, pp. 1697-1703.

[48] P.C.O. Silva, C. Nicolet, P. Grillot, J.L. Drommi, B. Kawkabani, Assessment of power swings in hydropower plants through high-order modelling and eigenanalysis, in: 2016 XXII International Conference on Electrical Machines (ICEM), IEEE, 2016, pp. 159-165.

[49] X. Liu, C. Liu, Eigenanalysis of oscillatory instability of a hydropower plant including water conduit dynamics, IEEE Transactions on Power Systems, 22 (2007) 675-681.

[50] H. Gao, X. Xie, J. Zhang, C. Wu, K. Sun, Second‐order oscillation mode study of hydropower system based on linear elastic model and modal series method, International Transactions on Electrical Energy Systems, (2016).

[51] R.C. Dorf, R.H. Bishop, Modern control systems, (1998).

[52] J. Bladh, Hydropower generator and power system interaction, in, Uppsala University, 2012.

[53] J. Lidenholm, U. Lundin, Estimation of hydropower generator parameters through field simulations of standard tests, IEEE Transactions on Energy Conversion, 25 (2010) 931-939.

[54] W. Zeng, J. Yang, W. Yang, Instability analysis of pumped-storage stations under no-load conditions using a parameter-varying model, Renewable Energy, 90 (2016) 420-429.

Highlights

A fundamental study on small signal stability of hydropower plants is conducted.

Hydraulic-mechanical-electrical coupling mechanism in hydropower system is studied.

A twelfth-order state matrix is developed for eigen-analysis.

Considerable influence from hydraulic-mechanical factors is shown.

Potential room on better parameter tunings (governor, AVR and PSS) is presented.